Short Telomeres Induce a DNA Damage Response in *Saccharomyces cerevisiae*

Arne S. IJpma and Carol W. Greider*

Department of Molecular Biology and Genetics, Graduate Program in Cellular and Molecular Medicine, The Johns Hopkins University School of Medicine, Baltimore, Maryland 21205

Telomerase-deficient *Saccharomyces cerevisiae* cells show a progressive decrease in telomere length. When grown for several days in log phase, the *tlc1*Δ cells initially display wild-type growth kinetics with subsequent loss of growth potential after which survivors are generated via *RAD52*-dependent homologous recombination. We found that chromosome loss in these telomerase-deficient cells only increased after a significant decline in growth potential of the culture. At earlier stages of growth, as the telomerase-deficient cells began to show loss of growth potential, the cells arrested in G2/M and showed *RNR3* induction and Rad53p phosphorylation. These responses were dependent on *RAD24* and *MEC1,* suggesting that short telomeres are recognized as DNA damage and signal G2/M arrest.

INTRODUCTION

The ends of linear chromosomes are protected by telomeres that consist of double-stranded repetitive sequences complexed with specific telomere-binding proteins. Each organism has a unique telomere length set-point. This set-point is the result of the balance between telomerase activity which extends the telomere (Greider and Blackburn, 1985) and activities that lead to shortening of the telomere such as DNA replication and nuclease activities (Reviewed in Greider, 1996). This equilibrium length maintenance results in a different number of telomere repeats on individual telomeres and heterogeneity in telomere length in a population of cells.

In the yeast *Saccharomyces cerevisiae*, telomeres consist of ~300 base pairs of TG1–3 repeats (Zakian, 1989). The catalytic components of *S. cerevisiae* telomerase are the telomerase reverse transcriptase Est2p (Lendvay *et al.*, 1996; Lingner *et al.*, 1997a, 1997b) and the RNA component *TLC1* (Singer and Gottschling, 1994). In addition, Cdc13p binds the single-stranded G-rich overhang of the telomere and is required to maintain telomere function (Garvik *et al.*, 1995; Lin and Zakian, 1996; Nugent *et al.*, 1996; Hughes *et al.*, 2000). Cdc13p recruits both telomerase via an interaction with Est1p (Evans and Lundblad, 1999; Qi and Zakian, 2000) and the telomere end-protection complex consisting of Stn1p and Ten1p to the telomere (Lin and Zakian, 1996; Nugent *et al.*, 1996; Grandin *et al.*, 1997, 2001; Pennock *et al.*, 2001).

* Corresponding author. E-mail address: cgreider@jhmi.edu.

Telomere function can be perturbed in two different ways. Immediate telomere dysfunction can be induced by disrupting the interaction between the telomere and telomere binding proteins (Garvik *et al.*, 1995; Kirk *et al.*, 1997; Karlseder *et al.*, 1999), whereas inhibition of telomerase activity with subsequent telomere shortening induces delayed telomere dysfunction (Lee *et al.*, 1998a; Hemann *et al.*, 2001a, 2001b).

Cells containing a temperature-sensitive allele of *CDC13* grown at the nonpermissive temperature arrest at the G2/M stage of the cell cycle in a *RAD9*-dependent process (Garvik *et al.*, 1995). In *Tetrahymena thermophila,* a mutant telomere sequence that prevents telomere binding proteins from interacting with the telomere, causes cells to accumulate in anaphase (Kirk *et al.*, 1997). In transformed and primary human cell-lines, overexpression of a dominant negative allele of the telomere binding protein TRF2 leads to p53 activation and p53- and ATM-dependent arrest or apoptosis (Karlseder *et al.*, 1999).

In *S. cerevisiae*, inactivation of telomerase results in progressive telomere shortening with accompanying loss of growth potential, chromosome instability, and cell death (Lundblad and Szostak, 1989; Hackett *et al.*, 2001). When the telomeres reach a critical short length, a recombination process mediated by Rad52p and other components leads to telomere elongation that allows a few cells to regain wild-type growth potential (Lundblad and Blackburn, 1993). These survivor cells subsequently reestablish the culture (Lundblad and Blackburn, 1993). Survivors fall into two classes: type I cells that show amplification of the telomere-associated Y′ elements and have very short TG1–3 repeat tracts and type II cells that have long variable tracts of TG1–3 repeats and only modest Y′ element amplification (Lundblad and Blackburn, 1993; Teng and Zakian, 1999). Type

I–mediated recombination depends on *RAD51, RAD54, RAD57, CDC13* and the replicative polymerases, whereas type II survivors depend on *RAD50, RAD59, MRE11, XRS2, TEL1,* and *MEC1* (Ritchie and Petes, 2000; Teng *et al.*, 2000; Chen *et al.*, 2001; Tsai *et al.*, 2002). Survivor generation is prevented by either deleting *RAD52* alone or deletion of any combination of genes that prevent both type I and type II survivor pathways (Le *et al.*, 1999).

In mice that lack the RNA component of telomerase (Blasco *et al.*, 1997), telomere dysfunction results in T-cell apoptosis, germ cell apoptosis, and testicular atrophy in late generation males (Lee *et al.*, 1998a; Hemann *et al.*, 2001a). Inactivation of p53 in the background of telomerase null mice decreases the degree of testicular atrophy, suggesting that p53 mediates the apoptotic response (Chin *et al.*, 1999). The apoptosis induced in the telomerase null mice is due to the shortest telomere to reach a minimal critical length (Hemann *et al.*, 2001b).

This short dysfunctional telomere may resemble a double-strand DNA break (DSB), which can activate a DNA damage response. DSBs induced by ionizing radiation or the HO endonuclease lead to a G2/M cell cycle arrest that allows time for repair of the damage (Weinert and Hartwell, 1988; Sandell and Zakian, 1993). In *S. cerevisiae*, the DNA damage response to a DSB is dependent on *RAD9, RAD24, RAD17, MEC3, DDC1, DDC2, MEC1, RAD53,* and *CHK2* (Lydall and Weinert, 1995, 1997; Zhou and Elledge, 2000; Melo and Toczyski, 2002; Rouse and Jackson, 2002). The DSB sensing complex is proposed to consist of *RAD24* in a complex with *RFC2, RFC3, RFC4,* and *RFC5*. This RFC-like complex might have a function similar to RFCs role of clamploader: recruiting the PCNA complex for initiation of DNA replication. This RFC-like complex recruits a PCNA-like complex consisting of Rad17p, Mec3p, and Ddc1p to the DSB (Shimomura *et al.*, 1998; Kondo *et al.*, 1999, 2001; Green *et al.*, 2000; Venclovas and Thelen, 2000; Melo *et al.*, 2001). This complex activates the signal transducing kinase Mec1p, which is a homolog of human ATR. Mec1p induces the phosphorylation of the effector kinases Rad53p, a homolog of human CHK2 (Allen *et al.*, 1994; Sanchez *et al.*, 1996; Sun *et al.*, 1996) and Chk1p, the homolog of human CHK1(Sanchez *et al.*, 1999).

Activation of Rad53p, which also depends on its interaction with Rad9p, leads to G2/M cell cycle arrest by preventing mitotic exit (Sun *et al.*, 1996, 1998; Charles *et al.*, 1998; Cheng *et al.*, 1998; Emili, 1998; Sanchez *et al.*, 1999; Soulier and Lowndes, 1999; Schwartz *et al.*, 2002). Rad53p also mediates activation of the kinase Dun1p, which controls the transcriptional induction of *RNR3*, a component of ribonucleotide reductase (Elledge and Davis, 1990; Gardner *et al.*, 1999).

The DSB-induced DNA damage response is also mediated by Tel1p, Mre11p, Rad50p, and Xrs2p. This pathway specifically responds to unprocessed DSBs in the absence of functional Mec1p (Usui *et al.*, 2001). The Mre11p, Rad50p, and Xrs2p (MRX) complex interacts with the DSB and activates the central kinase Tel1p. Tel1p subsequently activates Rad53p and Chk1p to establish G2/M arrest and to induce a DNA damage repair (D'Amours and Jackson, 2001; Grenon *et al.*, 2001; Usui *et al.*, 2001). Interestingly Tel1p, the MRX complex, and *MEC1* are also important in the recombination mediated process of type II survivor generation in telomer-

ase mutant cells (Le *et al.*, 1999; Ritchie and Petes, 2000; Teng *et al.*, 2000; Chen *et al.*, 2001; Tsai *et al.*, 2002).

To investigate the primary response to telomere shortening in *S. cerevisiae*, we examined the rate of chromosome loss, cell cycle arrest, and DNA damage response in telomerase-deficient yeast as these cells were losing growth potential. Chromosome loss occurred, as previously described (Lundblad and Szostak, 1989), however the increase in chromosome loss was only significant after the growth potential of the population reached a minimum. This suggests that chromosome instability is not the primary determinant of the initial loss of growth potential. As the telomerase mutant cells lost growth potential, they accumulated in the G2/M phase of the cell cycle, with Rad53p phosphorylation and *RNR3* mRNA upregulation. We propose that in *S. cerevisiae* in the absence of telomerase, short dysfunctional telomeres induce a DNA damage response, which subsequently leads to the loss of growth potential via a G2/M cell cycle arrest.

MATERIALS AND METHODS

Yeast strains constructions and growth media *S. cerevisiae* strains were grown as previously described (Rose *et al.*, 1990). All strains are derived from JHU500 (YPH983) *MATa/MATα ura3-52/ura3-52 lys2-801/lys2-801 ade2-101/ade2-101 his3Δ200/his3Δ200 trp1Δ1/ trp1Δ1 leu2Δ1/leu2Δ1 CFIII (CEN3.L.YPH983) URA3 SUP11* (kindly provided by Phil Hieter; Connelly and Hieter, 1996). The cells used in the chromosome loss assay carried the chromosome fragment. In all other experiments the chromosome fragment was not present. The strains used in this study are:*rad52Δ/RAD52*: JHU504(*MATa/ MATα rad52Δ::TRP1/RAD52)est2Δ rad52Δ/EST2 RAD52*: yAY139-(JHU504 *est2Δ::HIS3/EST2);tlc1Δ/TLC1:* JHU502(*MATa/MATα tlc1Δ:: LEU2/TLC1),tlc1Δ rad52Δ/TLC1 RAD52:* JHU508(JHU502 *tlc1Δ::LEU2/ TLC1),tlc1Δ rad9Δ/TLC1 RAD9:* yAY212(JHU502 *rad9Δ::KANMX4/ RAD9)tlc1Δ rad24Δ/TLC1 RAD24:* yAY103(JHU502 *rad24Δ::HIS3/ RAD24)tlc1Δ rad9Δ rad24Δ/TLC1 RAD9 RAD24:* yAY217(yAY212 *rad24Δ::HIS3/RAD24)tlc1Δ mad2Δ/TLC1 MAD2:* yAY120(JHU502 *mad2Δ::HIS3/MAD2)tlc1Δ mec1Δ sml1Δ/TLC1 MEC1 SML1:* yAY143(JHU502 *mec1Δ::HIS3/MEC1 sml1Δ::TRP1/SML1) tlc1Δ mec1Δ sml1Δ tel1Δ/TLC1 MEC1 SML1 TEL1:* yAY222(yAY143 *tel1Δ:: HPH/TEL1).* All gene disruptions were complete deletions of the open reading frames and were constructed by transforming the cells with either a plasmid-derived restriction fragment or a PCR-generated gene disruption fragment (Brachmann *et al.*, 1998) using the lithium acetate transformation method (Schiestl and Gietz, 1989). Gene disruptions were confirmed by restriction digest and subsequent Southern blotting. JHU502 was constructed by deleting *TLC1* in JHU500. JHU500 cells were transformed with *Xho*I-digested pBLUE61::LEU2 (Singer and Gottschling, 1994). JHU504 was constructed by transformation of *Bam*HI fragment from JH185 into JHU500. JH185 is pBR322 containing the *Bam*HI genomic fragment of *RAD52* (JH182 was obtained from David Schild) where the *Bgl*II/ *Bgl*II *RAD52* fragment is replaced by a *Bam*HI/*Bgl*II fragment containing *TRP1* from PRS316. *EST2* was deleted in JHU504 using a PCR product generated by AY10 (5'-AAGCATGGCAATGAATGA-CACAAGTGAAATAGAAAAGTGAGATTGTACTGAGAGTGCA-C-3') and AY11 (5'-CAGCATCATAAGCTGTCAGTATTTCATG-TATTATTAGTACTGTGCGGTATTTCACACCG-3') on PRS403 (Brachmann *et al.*, 1998). *RAD9* was deleted in JHU502 using a PCR product generated by AY41F (5'-CGGCCTTGTTAGCGTTAGAT-3') and AY41R (5'-GACCTTACCAACGTTGTTGG-3') on genomic DNA from haploid *rad9Δ::KANMX4* obtained from the *S. cerevisiae* Genome Deletion Project (Winzeler *et al.*, 1999). *RAD24* was deleted in JHU502 using a PCR product generated by:AY58F (5'-ATGGAT-AGTACGAATTTGAACAAACGCCCTTATTACAAAGATTGTA-CTGAGAGTGCAC-3') and AY58R (5'-TTAGAGTATTTCCA-GATCTGAATCTGAAAGGGACTCACTCTGT GC GG TA TT TCA-

CACCG-3′) on PRS403 (Brachmann *et al.*, 1998). *MAD2* was deleted in JHU502 using a PCR product generated by OLFS365 (5′-AGTA-ATTCCTTGGTCCACTG-3′) and OLFS366 (5′-GGTCAAAATTTGT-GAGGCAAG-3′) on genomic DNA of YFS1104/YPH1238 (kindly provided by Forrest Spencer; Hyland *et al.*, 1999). *MEC1* was deleted in JHU502 *sml1Δ::TRP/SML1* using a PCR product generated by AY37F (5′-CAAATAGATGGAACGCACGCTCCAAAACTAGTCA-ACTAGAGATTGTACTGAGAGTGCAC-3′) and AY37R (5′-AGC-CAACCAATATACATCTTGCTTAGATTGTCTTCTGATCTGTGC-GGTATTTCACACCG-3′) on PRS403 (Brachmann *et al.*, 1998). *SML1* was deleted in JHU502 using a PCR product generated by AY48F (5′-CTGCTCCTTTGTGATCTTACGGTCTCACTAACCTCTCTTA-GATTGTACTGAGAGTGCAC-3′) and AY39R (5′-CAATGTTG-GCGCTAGCGATATCTAGCTGTATCAAACGTACTGTGCGGTA-TTTCACACGC-3′) on PRS404 (Brachmann *et al.*, 1998). *TEL1* was deleted in yAY143 using a PCR product generated by AY130F (5′-GATGAGCTAACAACAATTTTAAAAGAAGATCCGGAAAGG-ATACCAAGATTGTACTGAGAGTGCAC-3′) and AY130R (5′-AAGCATCTGCATAGCAATTAATAAAAAGGTGACCATCCCA-GCATAGGCCACTAGTGGATCTG-3′) on pAG32 (Goldstein and McCusker, 1999). All deletion strains were always maintained as heterozygous diploids. All haploid deletion mutants used were generated by sporulation of the heterozygous diploids, followed by tetrad dissection and genotypic analysis of all the spores.

Chromosome Loss Assay

The chromosome loss assay was carried out as described (Spencer *et al.*, 1990). In this assay the loss of an artificial chromosome *CFIII (CEN3.L.YPH983) URA3 SUP11* is quantitated. This ~150-kb chromosome fragment, containing most of the left arm of chromosome III, is marked by the *URA3* gene and carries an ochre suppressor of the *ade2-101* allele, *SUP11*. The loss of this and similar chromosome fragments in wild-type cells is 1.7 chromosome loss events/10,000 mitosis (Hegemann *et al.*, 1988). In our sectoring assay only colonies that display half sectoring were counted as a chromosome loss event. In our assay, we kept the cultures in log phase while maintaining selection for the *URA3* gene on the chromosome fragment. After every five population-doublings, the cells were spread to single colonies on nonselective YPD plates. The five population doublings were obtained by measuring the starting concentration of the culture by hemacytometer and monitoring the population until the culture had reached a concentration of (starting concentration $\times 2^5$). For every time-point, a total of 20,000 colonies were analyzed for the appearance of half white/half red sectored colonies. Plating efficiency was normalized to the wild-type plating efficiency: ([actual colonies of sample on the plate/calculated number of cells spread on plate]/[actual wild-type colonies on the plate/calculated number of cells spread on plate])*100%.

Liquid Growth Potential Assay

Haploid cells of the appropriate genotypes were picked from a fresh dissecting plate after 48 h at 30°C and grown in yeast extract-peptone-dextrose (YPD) at a starting concentration of 1×10^4 cells/ml. Cells were kept in log phase for 17 h, and then the cell density was measured by counting cells in a hemacytometer (Bright-Line, Hausser Scientific, Horsham, PA). The culture was then diluted back to a density of 1×10^4 cells/ml. This cycle was repeated for 8–11 d. At all time points during growth, cells were examined for possible contamination. Every day, the concentration of the culture after 17 h of growth was plotted on a curve. This curve represents the growth potential of the different mutants. Wild-type cells when started at 1×10^4 cells/ml reach a maximum concentration of 5×10^7 cells/ml after 17 h of growth. For all liquid growth potential experiments, all haploid cells compared within one experiment were derived from sporulation of one parent diploid strain.

Cell Viability Assay

To measure cell viability, the cells were grown for 4 h in YPD medium containing phloxin at a concentration of 20 μg/ml (Schupbach, 1971; Kohli *et al.*, 1977). This dye enters metabolically dead cells and therefore can be used to quantitate percent of dead cells in a population. For every data-point, 2000–2500 cells were analyzed in a hemacytometer for the presence of red cells.

Individual Cell Growth Rate Assay on Plates

Cells from various time points during the growth potential assay were plated onto YPD plates and allowed to grow for 6 h. The growth rate during this time was measured by capturing an image directly after plating the cells and again at 6 h after growth at 30°C. Images were acquired at 400× magnification using a Zeiss Axioskop and images were captured with a CCD camera (Photometrix Sensys) and processed with IP-Lab Spectrum acquisition software (Scanalytics). The number of divisions was then calculated by a comparison of the two images. Only cells that started as a single cell, a doublet, or triplet were measured.

Division number was calculated as follows: For the single cells, after 6-h growth, a single cell was counted as 0 divisions, increase to 2–3 cells was counted as 1 division, increase to 4–6 cells was counted as 2 divisions, increase to 7–12 cells was counted as 3 divisions, and increase to 13 or more was measured as 4 divisions. For the doublets, after 6 h growth, 2–3 cells was counted as 0 divisions, increase to 4–6 cells was counted as 1 division, increase to 7–12 cells was counted as 2 divisions, increase to 13–24 cells was counted as 3 divisions, and increase to 25 or more was measured as 4 divisions. For the triplets, after 6 h growth, 3 or 4 cells was counted as 0 divisions, increase to 5–9 cells was counted as 1 division, increase to 10–18 cells was counted as 2 divisions, increase to 19–36 cells was counted as 3 divisions and increase to 37 or more was measured as 4 divisions. 60 microcolonies were analyzed for every time point.

Cell Cycle Stage Quantitation

Cell cycle stage quantitation was performed on DAPI-stained cells, using fluorescence microscopy. Cells from log phase cultures were fixed in 70% ethanol. After rehydration the cells were resuspended in 0.5 mg/ml DAPI in 10% glycerol and mounted on a slide. For quantitation purposes, the cells were divided into four stages: G1/S, S/G2, G2/M, and M/G1, based on morphology (Hartwell, 1974). Images were acquired at ×1000 magnification using a Zeiss Axioskop, and images were captured with a CCD camera (Photometrix sensys) and processed with IP-Lab Spectrum acquisition software (Scanalytics). Some cells were not quantifiable; those were put into a separate group, termed "others." Single unbudded cell with one nucleus, were designated as G1/S, a mother cell with a small bud and nucleus close to budneck was designated S/G2, a mother cell with equal sized daughter and nucleus at budneck was designated G2/M, and mother cell with smaller or equal sized daughter, each containing one nucleus, was designated M/G1 cells. For every time-point at least 250 cell-bodies were counted. For cell cycle quantitation experiments, all haploid cells compared within one experiment were derived from sporulation of one parent diploid strain. The data for each mutant is derived from the analysis of one mutant spore, which is representative for the multiple isolates of the same genotype analyzed. In these experiments only comparisons between haploid genotypes that were sporulated from a given multiple heterozygous diploid were made, because the starting telomere length may differ in the independent experiments. In addition, although the results for independent spores with the same genotype within an experiment were qualitatively very similar, there still was spore to spore variation in the timing of onset of loss of growth potential and appearance of survivors.

Total RNA blot analysis

Cells from log phase cultures from different days of the growth potential assay were frozen on dry ice and ethanol and stored at −80°C. Total yeast RNA was prepared by a hot acidic phenol extraction method (Collart and Oliviero, 1993). RNA concentration was measured using GeneSpecI spectrophotometer (Hitachi). Twenty-five micrograms of total RNA was fractionated in a formaldehyde agarose (1%) gel and subsequently transferred to a Hybond-N$^+$ nylon membrane (NEN Life Science Products) in 10× SSC. The RNA was cross-linked to the filter by UV irradiation in a UV Stratalinker 2400 (Stratagene). Probes were made by random-primed labeling using Klenow enzyme (New England Biolabs) and [α-^{32}P]dGTP and [α-^{32}P]dATP (NEN Life Science Products) at 30°C for 4 h (Feinberg and Vogelstein, 1983). The actin-specific probe template spans the *ACT1* coding region from nucleotide 339 to nucleotide 1421. It was amplified using AY43F-2 (5'-GATAACGGT-TCTGGTATG-3') and AY43R (5'-GGTGAACGATAGATGGACCA-3') using yeast genomic DNA as a template. The *RNR3* probe template spans the *RNR3* coding region from nucleotide 51 to nucleotide 1532. It was amplified using AY42F (5'-ATTACCTC-CCGTATCACCCG-3') and AY42R (5'-ACCCTGGACACCAAGAG-CAA-3') using yeast genomic DNA as template. Before adding to the formamide hybridization solution, labeled probes were purified from unincorporated [α-^{32}P]dNTP using NAP^{TM}5 columns (Pharmacia Biotech). Hybridization was performed at 42°C for 16 h. The filters were washed in 0.1 × SSC/0.1% SDS at 42°C three times for 20 min. Quantitation was performed using a BAS1500 phosphoimager (Fujifilm) and Image Quant (Molecular Dynamics) software.

Western Analysis

For each sample, 3×10^8 cells from log phase cultures from different days of the growth potential assay were frozen on dry ice and ethanol and stored at −80°C. Protein extract was prepared using the glass bead lysis method. The cell pellet was thawed and resuspended in yeast lysis buffer (50 mM Tris, pH 7.5, 1% SDS, 5 mM EDTA, 0.001% β-mercapto-ethanol) containing protease and phosphatase inhibitors. Glass beads were added to the meniscus and the cells were vortexed 4–5 times for 30 s pulses with 1 min on ice in between the pulses to keep the samples cold. Next the lysate was boiled for 3 min after which 50 μl of fresh YLB was added with subsequent vortexing. The sample was centrifuged at 4°C for 20 min. Then the lysate was transferred to a new tube and protein concentration was determined by the Bradford assay in a UV160U spectrophotometer (Shimadzu). Forty micrograms of total protein extract was fractionated on a 8% SDS-polyacrylamide (SDS-PAGE) gels, and transferred to PVDF Immobilin-P membranes (Millipore) using the TRANS-BLOT SD semi-dry transfer cell (Bio-Rad). The protein blot was incubated for 12 h at 4°C with goat polyclonal IgG anti-Rad53p (Santa Cruz) at 1:300 dilution in 5% milk TTBS (100 mM Tris, pH 7.5, 2.7 mM KCl, 137 mM NaCl, 0.1% Tween-20). After washing in TTBS, the blot was incubated with rabbit anti-goat HRP IgG (H+L; Jackson Immunoresearch) 1:10,000 dilution in 5% milk TTBS for 1 h at room temperature. After washing in TTBS, the signal was generated using ECL Western blotting detection reagents (Amersham Pharmacia Biotech). The signal was detected using X-OMAT AR film (Kodak) developed in M35A X-OMAT processor (Kodak).

RESULTS

Chromosome Loss and Cell Death Do Not Account for the Decrease in Growth Potential in Telomerase-deficient Cells

When telomerase mutants are grown in culture, telomere shortening is apparent in the first few divisions, however, cell growth potential is normal until about the 40th division, when a decline in growth potential is seen (Lundblad and

Szostak, 1989; Singer and Gottschling, 1994). The term "loss of growth potential" is introduced here to describe the difference in growth of the telomerase mutant and the wild-type culture and is neutral with regard to the mechanistic basis of this poor growth. This decrease in growth potential, previously termed senescence, has been attributed to loss of telomere function followed by chromosome instability and subsequent cell death (Lundblad and Szostak, 1989).

To investigate the role of chromosome instability in the loss of growth potential in telomerase mutants in more detail, we carried out a quantitative chromosome loss assay (Hieter *et al.*, 1985; Spencer *et al.*, 1990). Telomerase was inactivated by deleting *EST2* encoding the catalytic protein component of telomerase. The *est2Δ* strain contained a non-essential 150-kb artificial chromosome that carries most of the left arm of chromosome III and the *SUP11* gene, which encodes a tRNA that suppresses the ochre mutation of *ade2-101* (Spencer *et al.*, 1990). Colonies with an *ade2-101* mutation that carry the suppressor are white; however, loss of the chromosome with *SUP11* results in red colonies. With this strain, chromosome loss can be quantitated by measuring the red sectoring in white colonies. Half-sectored colonies represent loss of the artificial chromosome at the first division of a single cell (Hieter *et al.*, 1985). We grew the telomerase mutant cells in liquid culture while maintaining selection for the artificial chromosome. Every five population doublings, we plated the cells on nonselective plates and counted the number of half-sectored colonies in a total of 20,000 colonies (Figure 1B). At the same time the growth potential was measured by monitoring the plating efficiency of the cells (Figure 1A).

Hegemann *et al.* (1988) determined that the loss of the chromosome fragment in wild-type cells was 1.7 chromosome loss events/10,000 mitosis. We found a similar average chromosome loss of 1.9 loss events/10,000 mitosis in our wild-type cells. Chromosome loss in the *est2Δ* cells was comparable to that of wild-type cells for the first 50 generations. Chromosome loss of the *est2Δ* cells only increased to threefold higher than that of the wild-type cells by the time the *est2Δ* population displayed a decreased growth potential at generation 60. The chromosome loss was maximal when the growth potential was at a minimum at 75 generations, at which point the *est2Δ* cells displayed a 17-fold higher chromosome loss than the wild-type cells. *tlc1Δ* cells showed a similar increase in chromosome loss compared with *est2Δ* cells (our unpublished results). *rad52Δ* cells, which are known to have a high chromosome loss (Mortimer *et al.*, 1981; Sandell and Zakian, 1993), had a five- to eightfold higher chromosome loss than wild-type cells throughout the experiment and did not show a progressive decrease in growth potential. The chromosome loss in the *est2Δ* culture was less than the loss in *rad52Δ* cultures for the first 70 generations, although the *est2Δ* cells lost growth potential and the *rad52Δ* cells did not. This suggests that that increased chromosome loss is not solely responsible for the decreased growth potential of *est2Δ cells.*

We next tested whether the loss of growth potential correlated with an increased rate of cell death. Cell viability was measured directly by assaying the percent of cells that stain with phloxin (Figure 2). Phloxin dye only enters cells that are metabolically dead (Schupbach, 1971; Kohli *et al.*, 1977). All cells were grown in log phase culture for 10 d and the
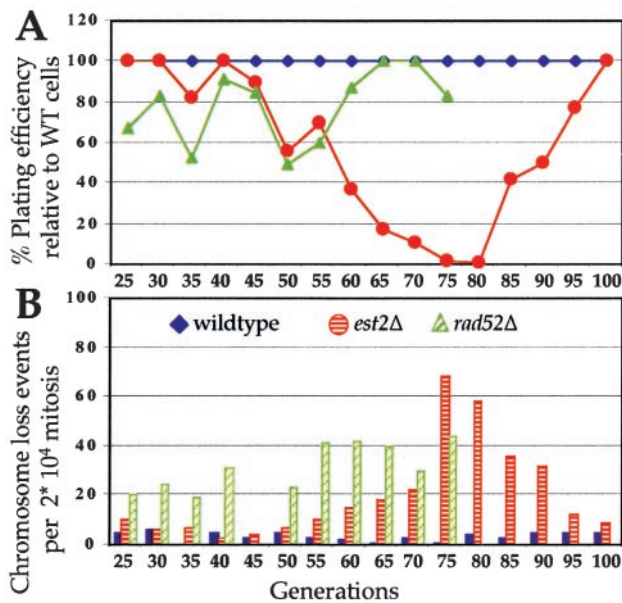
Figure 1. Chromosome loss and plating efficiency of wild-type, *est2Δ* and *rad52Δ* cells. (A) The plating efficiency of all cells was measured and was normalized to the wild-type plating efficiency. For plating efficiency, wild-type is denoted as blue diamonds, *est2Δ* as red circles and *rad52Δ* as green triangles. (B) Chromosome loss was measured in the wild-type, *est2Δ*, and *rad52Δ* cultures. Wild-type is denoted as blue filled bars, *est2Δ* as red horizontally striped bars, and *rad52Δ* as green hatched bars. The *rad52Δ* cells were only grown until generation 75 because of a loss of function mutation in the *SUP11* gene after this point. No chromosome loss data was generated for wild-type cells at generation 35 and for *rad52Δ* cells at generation 45.

Figure 2. Cell viability of wild-type and *tlc1Δ* cells in the growth potential assay. (A) Wild-type (black lines) and *tlc1Δ* (gray lines) cells were grown in log-phase for 11 d. Every day the growth potential of the cultures was measured. For each genotype four independent isolates were analyzed. (B) The percent of phloxin positive cells was plotted for wild-type (black line) and *tlc1Δ* cells (gray line) derived from the corresponding days of the growth potential assay in A.

growth potential of *tlc1Δ* and wild-type cells was monitored each day (Figure 2A). Cells were kept in log-phase by starting the cultures at a concentration of 1×10^4 cells/ml. The cultures were then grown for 17 h during which time the wild-type cells reach a concentration of 5×10^7 cells/ml. Cells with reduced growth potential reached lower concentrations after 17 h of log-phase growth. The cell concentration was measured after growth for all cultures and the cells were rediluted to 1×10^4 cells/ml and grown for another 17 h. We will refer to this assay as the growth potential assay. The increase in the average population doubling time in this assay correlated well with the decrease in colony forming units shown in Figure 1A .

To measure viability, each day an aliquot of the cells was tested for phloxin staining (Figure 2B). Four independent wild-type and four independent *tlc1Δ* cultures were tested. Wild-type cells grown for several days in liquid culture showed no decline in growth potential and no phloxin staining. In *tlc1Δ* cultures there was an increase in phloxin staining as the growth potential declined. At day 4 of the growth potential assay, 2% of the *tlc1Δ* cells stained with phloxin. On day 6 or 7, when *tlc1Δ* cells were at the lowest point of the growth potential assay, only between 5 and 12% of the *tlc1Δ* cells stained with phloxin. If cell death were the direct cause for the decreased growth potential, a much higher cell death rate would be expected. These results suggest that
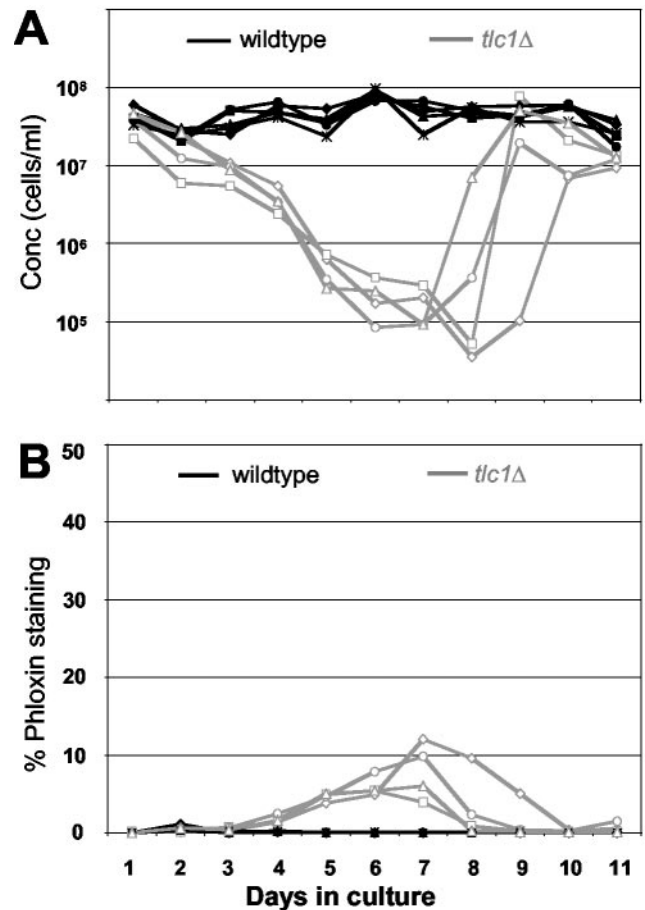
most of the cells that have stopped growing in a *tlc1Δ* culture are still metabolically viable.

Individual Telomerase Mutant Cells Show Decreased Growth Rate

Growth of cells in liquid culture only gives information on the mean growth potential of the population. To evaluate the growth rate of individual cells, we measured the growth rate of wild-type and *tlc1Δ* cells in a microscopic assay. After each day of growth in liquid culture (Figure 3A), single cells were plated on YPD plates and examined for their ability to form microcolonies (Figure 3B). The number of divisions that each individual cell underwent was monitored during a 6-h time span (Figure 3C). Most wild-type cells divided three times during this time. On the first day of growth, most of the *tlc1Δ* cells also divided three times. However starting at day 3, 80% of *tlc1Δ* cells divided only 0–2 times
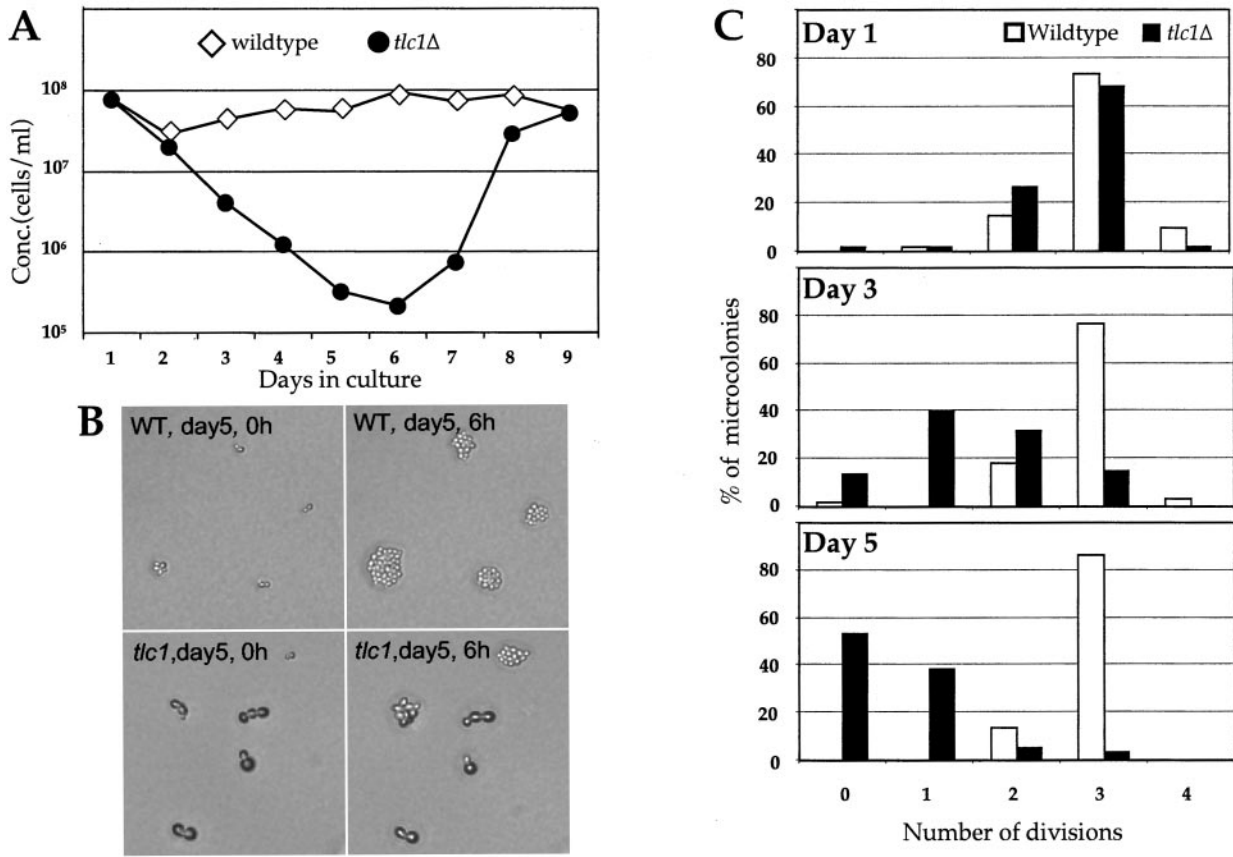
Figure 3. Individual telomerase mutant cells show decreased growth potential. (A) The growth potential assay was carried out for wild-type ($\Diamond$) and *tlc1Δ* ($\bullet$) cultures. (B) Wild-type and *tlc1Δ* cells from day 5 of the growth potential assay were plated out and incubated at 30°C for 6 h. Pictures were taken at the beginning (0 h) and the end (6 h) of the experiment. (C) Quantitation of the growth potential of individual wild-type ($\square$) and *tlc1Δ* ($\blacksquare$) cells. The increase in cell number in the microcolonies in the 6-h time span was counted and converted to total number of divisions. All images were captured at 400× magnification.

and by day 5; 90% of *tlc1Δ* cells did not divide at all or divided only once. Fifty percent of *tlc1Δ* cells were not dividing at day 5, which is significantly higher than the 12% phloxin-positive cells in the viability assay, suggesting that most nondividing cells were arrested rather than dead. The heterogeneity in the timing of the arrest of individual cells is likely due to the heterogeneity of the initial telomere length in the population.

Telomerase-deficient Cells Accumulate in the G2/M Phase of the Cell Cycle

To examine whether the loss in growth potential is caused by a cell cycle arrest, the distribution of cells at specific cell cycle stages was examined microscopically. Wild-type and *tlc1Δ* cells were grown in log phase for 9 d (Figure 4A). Cells were examined at days 1, 3, and 5 when the culture was losing growth potential. With increasing days of growth in liquid culture, the *tlc1Δ* cells accumulated as dumbbell-shaped cells with the nucleus in the bud neck. In addition the *tlc1Δ* cells increased in size as the growth potential of the culture declined. Both the G2/M accumulation and the cell

size increase were dependent on the DNA damage checkpoint gene *RAD24* (Figure 4B). Next, a quantitative assay was performed to measure the amount of G2/M arrest by counting the number of cells in four defined cell cycle stages. Each day the number of unbudded cells (G1/S), cells with small buds (S/G2), dumbbell-shaped cells with one nucleus (G2/M), and dumbbell-shaped cells with two nuclei (M/G1; Hartwell, 1974) were quantitated (Figure 5, A and B). The results from one isolate for each genotype are shown. However each genotype was analyzed multiple times and similar results were obtained in the independent experiments (see MATERIALS AND METHODS). The wild-type cultures displayed a distribution of G1/S (15–20%), S/G2 (55–65%), and M/G1 (10–25%), with only a small fraction (2–4%) of the cells in G2/M for all days (Figure 5B and unpublished data). The wild-type cells retained normal cell size throughout the experiment. In contrast, the *tlc1Δ* cells only had a cell cycle distribution and cell size similar to that of wild-type cells on the first day of growth. On day 4, the *tlc1Δ* culture contained 38% cells in G2/M and on days 5 and 6, these numbers were 52 and 58%, respectively (Figure 5B). Most of these G2/M-arrested cells were large-sized cells (Figure 4B and unpub-
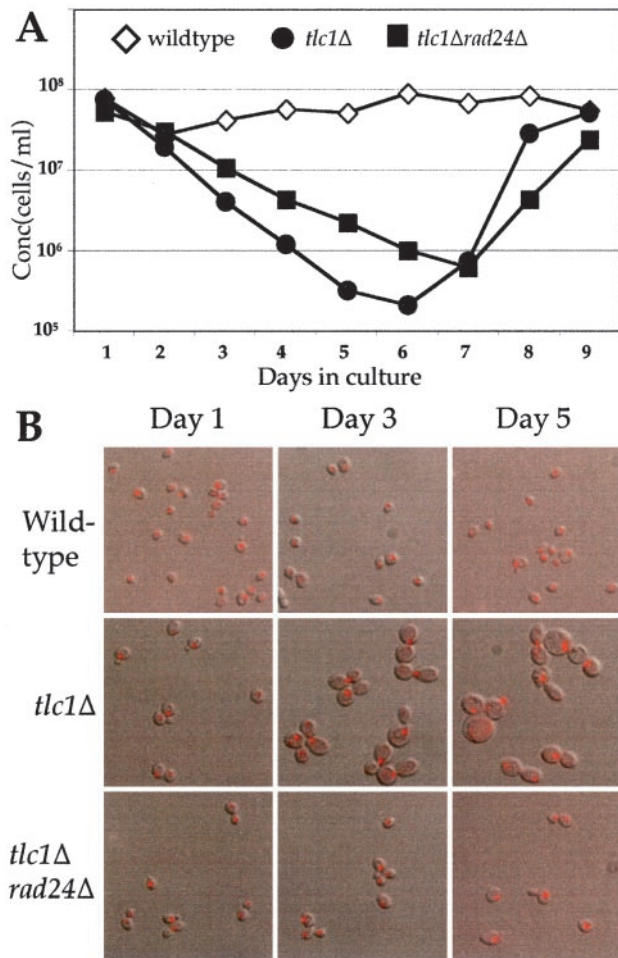
Figure 4. Telomerase-deficient cells accumulate in the G2/M phase of the cell cycle. (A) A growth potential assay was carried out for wild-type (◇) and *tlc1Δ* (●) and *tlc1Δ rad24Δ* (■). (B) DAPI (red) stained wild-type, *tlc1Δ* and *tlc1Δ rad24Δ* cells from days 1, 3, and 5 of the growth potential assay. All images were captured at the same (×1000) magnification.

lished data). At day 10, after survivors were generated, the *tlc1Δ* cells reverted to wild-type cell size and showed a cell cycle distribution similar to wild-type cells. These results show that an increasing proportion of *tlc1Δ* cells arrest at G2/M as telomeres undergo progressive shortening. The increase in cell size could be due to continued metabolic growth of the arrested cells.

Accumulation of G2/M-arrested Cells in Response to Short Telomeres Depends on **RAD24** and **MEC1**

To examine if the G2/M arrest in *tlc1Δ* cells was mediated by a DNA damage checkpoint, the requirement of specific checkpoint genes for this arrest was tested. The cell cycle distribution of mutants deleted for *TLC1* in combination with either *rad9Δ, rad24Δ, rad9Δ rad24Δ, mec1Δ, tel1Δ,* or *mad2Δ* was investigated. As described above, *tlc1Δ* cells showed an increase in the number of G2/M-arrested cells. In

contrast, the *tlc1Δ rad24Δ* double mutants showed a significant reduction in the number of arrested cells at all points in the growth potential assay (Figures 5B). Although there still remained a fraction of G2/M-arrested cells in the *tlc1Δ rad24Δ* mutants, these were predominantly normal-sized cells. A less pronounced reduction in G2/M-arrested cells was seen when the *tlc1Δ* mutant was compared with the *tlc1Δ rad9Δ* cells (Figures 5B). However, the *tlc1Δ rad9Δ* cells showed a similar decrease in large cells compared with the *tlc1Δ rad24Δ* mutants (our unpublished results). Deletion of both *RAD9* and *RAD24* in the *tlc1Δ* cells, again resulted in a reduction of G2/M-arrested cells, similar to that observed in the *tlc1Δ rad24Δ* double mutants (Figure 5B).

The role of *MEC1* and *TEL1* in the short telomere mediated cell cycle arrest was also investigated (Figures 6 and 7). Inactivation of *MEC1* in a *tlc1Δ* mutant, abrogated the G2/M arrest (Figure 6, A and B). However, a deletion of *TEL1* did not significantly change the cell cycle distribution in the *tlc1Δ* cells (Figure 7, A and C). These results imply that the cell cycle arrest is mediated, at least in part, by *RAD9, RAD24,* and *MEC1.*

In *Tetrahymena thermophila*, a mutant telomere sequence disrupted telomere length maintenance and resulted in the accumulation of cells in anaphase, possibly because of a problem in chromosome segregation (Kirk *et al.*, 1997). To investigate the role of the spindle checkpoint in the observed G2/M arrest, *MAD2* was deleted in the *tlc1Δ* cells. Quantitation of the cell cycle stages revealed no difference between the *tlc1Δ* and *tlc1Δ mad2Δ* cells (Figure 7, B and D). Thus, the spindle checkpoint does not play a major role in the accumulation of *tlc1Δ* cells at G2/M.

Short Telomeres Induce an Increase in **RNR3** *mRNA* and Rad53p Phosphorylation

To further examine whether short telomeres activate a DNA damage checkpoint, we examined the induction of *RNR3* mRNA and Rad53p phosphorylation. The same samples analyzed for cell cycle distribution (Figure 4) were analyzed for *RNR3* mRNA expression. There was an increase in the *RNR3* mRNA beginning at day 3 in *tlc1Δ* cells (Figure 8A). As the number of G2/M-arrested cells increased (see Figure 4, A and B), the *RNR3* mRNA expression level reached a maximum on day 5 (Figure 8A). This increase in *RNR3* was not seen in the *tlc1Δ rad24Δ* double mutant (Figure 8B; see also Figure 4, A and B), indicating that the upregulation of the *RNR3* mRNA is due to a *RAD24*-dependent DNA damage checkpoint response.

We next tested whether Rad53p was phosphorylated in *tlc1Δ* cells. Rad53p phosphorylation can be measured by the appearance of slower migrating species of Rad53p on a Western blot (Allen *et al.*, 1994; Sanchez *et al.*, 1996; Sun *et al.*, 1996). Rad53p is phosphorylated in response to treatment with methyl methanesulfonate (MMS), ionizing radiation, and HO-endonuclease–induced DSB formation (Allen *et al.*, 1994; Sanchez *et al.*, 1996; Sun *et al.*, 1996; Pellicioli *et al.*, 1999). When wild-type yeast cells were treated with MMS or bleomycin, a DSB-inducing agent (Grenon *et al.*, 2001), the slower migrating species of Rad53p were observed (Figure 8C and our unpublished results). These slower migrating species disappeared upon calf intestinal phosphatase treatment, indicating that the shift in migration is due to phosphorylation (our unpublished results). After 1 day of growth
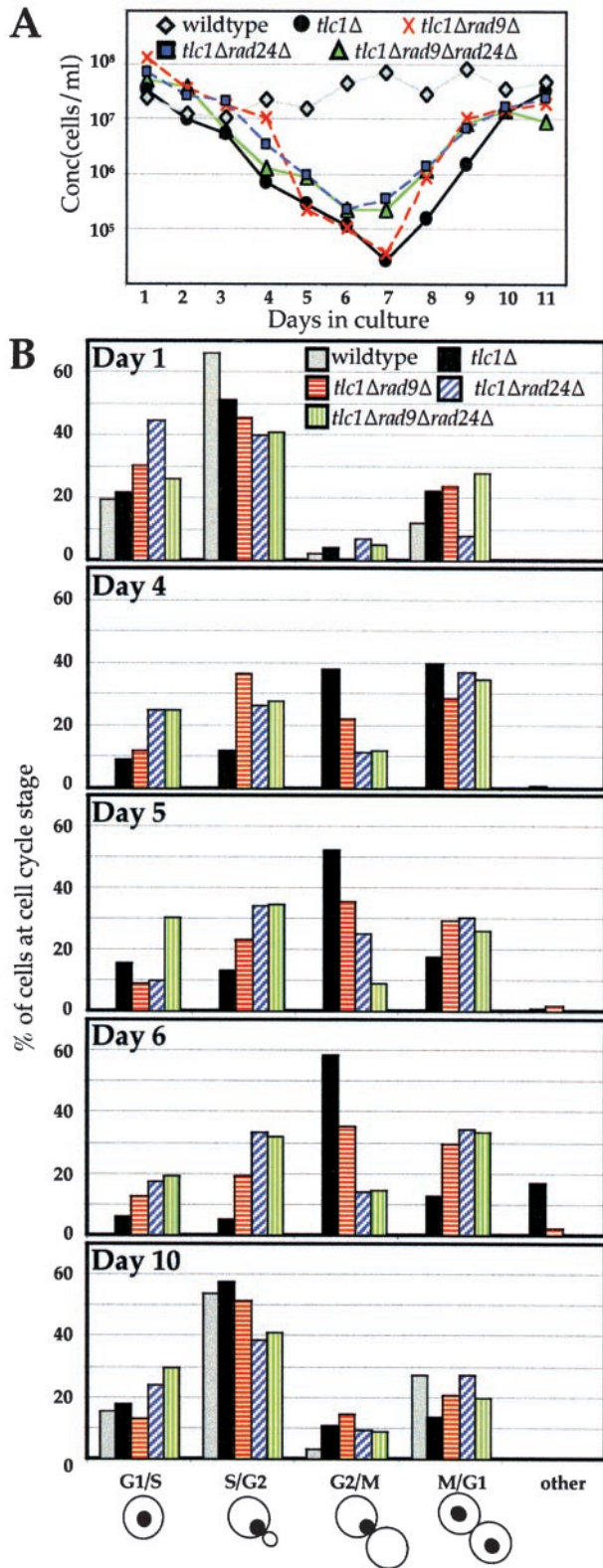
in culture, Rad53p was unphosphorylated in *tlc1Δ* cells; however, at day 5, the phosphorylated form of Rad53p was seen. Inactivation of *RAD9* in the *tlc1Δ* cells resulted in a complete loss of Rad53p phosphorylation, whereas inactivation of *RAD24* in the *tlc1Δ* cells decreased the level of Rad53p phosphorylation but did not abolish it (Figure 8C). The *tlc1Δ rad9Δ rad24Δ* triple mutant displayed complete loss of Rad53p phosphorylation similar to the *tlc1Δ rad9Δ* cells. In addition a *tlc1Δ mec1Δ sml1Δ* triple mutant strongly reduced the Rad53p phosphorylation, whereas the *tlc1Δ sml1Δ* double did not. These experiments show that *tlc1Δ* cells arrest in the G2/M phase of the cell cycle due to a *RAD24*, *MEC1*–dependent DNA damage response.

DISCUSSION

Telomere Dysfunction Due to Short Telomeres Initiates a G2/M Checkpoint Arrest

Double-strand DNA breaks induce a cell cycle arrest as a mechanism to allow DNA repair before proceeding with cell division (Weinert and Hartwell, 1988). In mammalian cells, short telomeres or a loss of telomere structure can activate a checkpoint response that results in cell cycle arrest or apoptosis (Lee *et al.*, 1998a; Karlseder *et al.*, 1999; Hemann *et al.*, 2001a). This checkpoint response requires p53 (Chin *et al.*, 1999; Karlseder *et al.*, 1999) and in some cases ATM (Karlseder *et al.*, 1999). This suggests that, when telomere function is lost, the chromosome end is sensed by the cell as a double-strand DNA break and activates a checkpoint response (reviewed in Hemann *et al.*, 2000; de Lange, 2002).

In yeast cells, experiments have shown that loss of telomere function leads to chromosome loss, chromosome rearrangements and chromosome end-to-end fusion (Lundblad and Szostak, 1989; Sandell and Zakian, 1993; Hackett *et al.*, 2001). Cell cycle arrest occurs in yeast in response to DNA damage such as double-strand breaks (Weinert and Hartwell, 1988; Sandell and Zakian, 1993). In addition there is evidence that telomere dysfunction may induce a cell cycle checkpoint (Garvik *et al.*, 1995; Lydall and Weinert, 1995; Ritchie *et al.*, 1999; Johnson *et al.*, 2001). To examine whether chromosome loss or cell cycle arrest is the major contributor to the decreased growth potential in the absence of telomerase, we used a quantitative assay to measure chromosome loss rates. After the initiation of telomere shortening by

Figure 5. Accumulation of G2/M-arrested cells in *tlc1Δ* cells depends on *RAD24* and to a lesser extent on *RAD9*. (A) Growth potential assay for wild-type (gray diamonds), *tlc1Δ* (black circles), *tlc1Δ rad9Δ* cells (red X), *tlc1Δ rad24Δ* cells (blue squares) and *tlc1Δ rad9 Δrad24Δ* (green triangles) (B) Quantitation of cell cycle distribution of DAPI-stained cells. Wild-type (gray bars), *tlc1Δ* (black bars), *tlc1Δ rad9Δ* (horizontally red striped bars), *tlc1Δ rad24Δ* (hatched blue bars) and *tlc1Δ rad9Δ rad24Δ* (vertically striped green bars) cells were divided into different cell cycle stages as described in the materials and methods and as depicted at the bottom of the graphs. Wild-type cells are only shown for first and last day of experiment but showed similar profiles for days 4, 5, and 6. The data for each mutant is derived from the analysis of one mutant spore that is representative for the multiple isolates analyzed. For each mutant three independent isolates were analyzed; for the *tlc1Δ rad9Δ rad24Δ* mutant two independent isolates were analyzed.
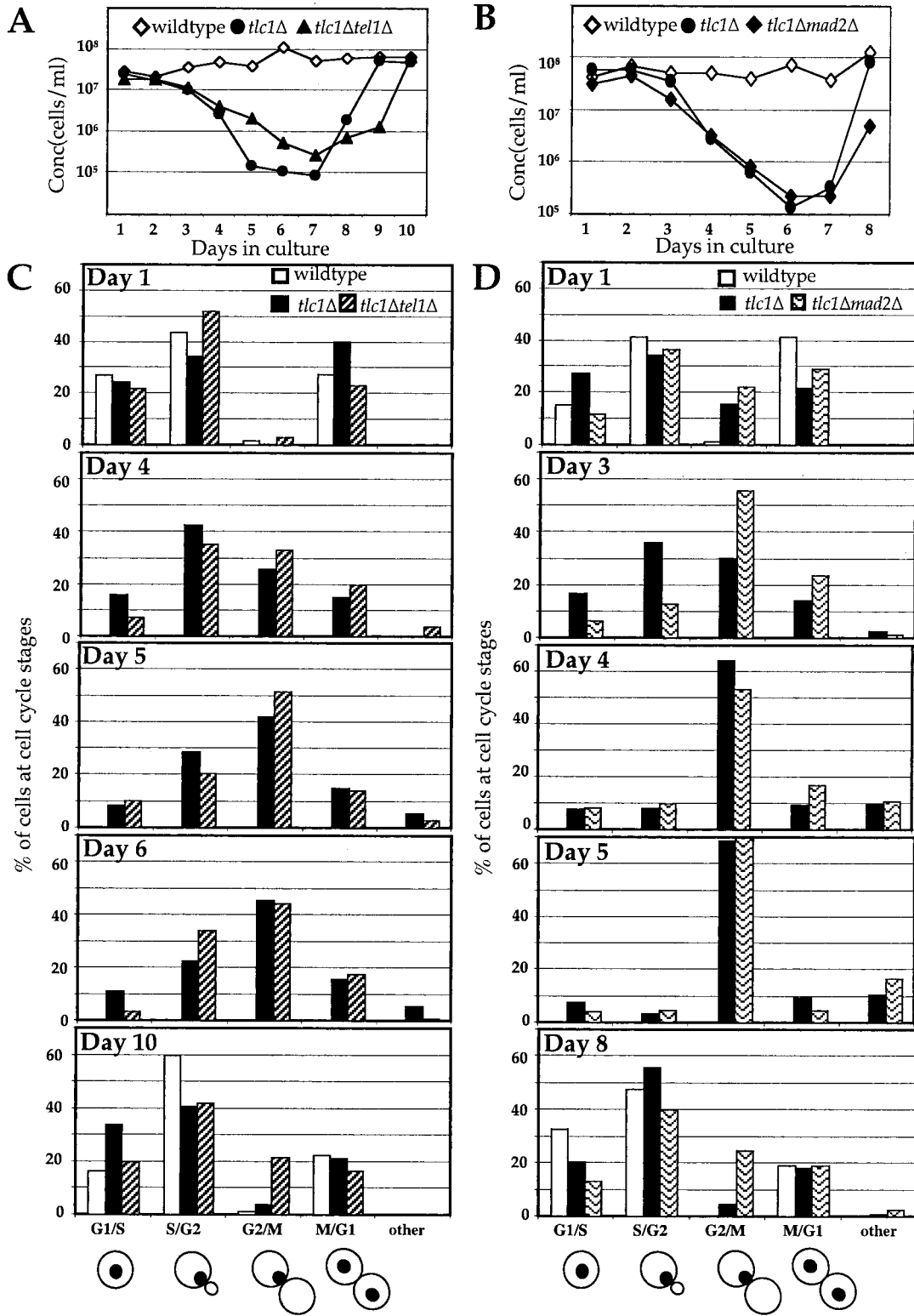
Figure 6. Accumulation of large G_2/M-arrested cells in *tlc1Δ* cells depends on *MEC1*. (A) Growth potential assay for wild-type (◇), *tlc1Δ* (●) and *tlc1Δ mec1Δ sml1Δ* cells (▲). (B) Quantitation of cell cycle distribution of DAPI-stained cells. Wild-type (white bars), *tlc1Δ* (black bars) and *tlc1Δ mec1Δ sml1Δ* (dotted bars) cells. Cells were divided into different cell cycle stages as depicted at the bottom of the graphs. *SML1* was also deleted in these cells to rescue the lethality of a *MEC1* deletion. Deletion of *SML1* in the background of *tlc1Δ* did not change the G2/M cell cycle arrest. Wild-type cells are only shown for first and last day of experiment but showed similar profiles for days 4, 6, and 7. The data shown for each mutant is derived from the analysis of one mutant spore. Another isolate that was analyzed for each mutant gave similar results.

telomerase inactivation, chromosome loss occurred, but the amount of loss did not explain the decreased plating efficiency of the *est2Δ* population. In contrast, the fraction of G2/M-arrested cells did correlate with the loss of growth in a telomerase null culture.

Inactivating components of the checkpoint pathway, *RAD9, RAD24,* and *MEC1* resulted in loss of the DNA damage response and decreased cell cycle arrest; thus, we conclude that loss of growth potential in a telomerase null culture is primarily due to a DNA damage-induced G2/M cell cycle arrest. This damage response could be a direct response to short telomeres or a response to breaks induced by chromosome fusions.

RAD24 and *MEC1* are required for the cell cycle arrest response to short telomeres, whereas *RAD9* plays a minor role in mediating the arrest. In contrast, deletion of *RAD9* dramatically reduced Rad53p phosphorylation, whereas a deletion of *RAD24* gave only partial reduction in phosphorylation. This suggests that telomere damage signaling might occur via kinases downstream of *RAD24* and *MEC1* and that the interaction between *RAD9* and *RAD53* is not essential for this process. It was previously shown that *RAD9* and *RAD24* have a similar contribution to the damage response in the temperature-sensitive mutant *cdc13-1* at nonpermissive temperature (Lydall and Weinert, 1995). This might indicate that the damage response to a telomere of wild-type length that abruptly loses end protection via the loss of Cdc13p is subtly different from the damage response to short telomeres. *RAD9* and *RAD24* single mutants are known to act somewhat synergistically in their response to DNA damage in several experimental settings such as response to UV irradiation. A more severe loss of G1/S and G2/M arrest responses is often seen when both genes are mutated together (Eckardt-Schupp *et al.*, 1987; Lydall and Weinert, 1995; de la Torre-Ruiz *et al.*, 1998). However, our results indicate that telomere damage is mainly sensed via *RAD24* because the *tlc1Δ rad24Δ* mutants and the *tlc1Δ rad9Δ rad24Δ* mutants show a very similar loss of the G2/M-arrested cells.

While this article was under review, Enomoto *et al.* (2002) published similar results showing a G2/M arrest in response to short telomeres. They showed that the G2/M arrest was dependent on *RAD24, MEC3, DDC2,* and *MEC1*, whereas *RAD9, TEL1,* and *RAD53* did not play a role in this arrest, consistent with our results. One apparent difference with our results is that the deletion of *RAD53* did not change the G2/M arrest in the Enomoto *et al.* experiments, whereas we find strong induction of Rad53p phosphorylation in response to short telomeres. These results can both be ex-

Figure 7.

plained because the damage signal from Mec1p is transduced to two parallel downstream kinases Rad53p and Chk1p that have additive functions in mediating arrest (Gardner *et al.*, 1999; Sanchez *et al.*, 1999).

Multiple Dysfunctional Telomeres May Not Allow Adaptation

Checkpoint arrest induced by DNA-damage is thought to be a response that allows cells time to repair the damage before proceeding in the cell cycle (Weinert and Hartwell, 1988). One unrepaired double-stranded break created by induction of the site-specific HO-endonuclease in a disomic haploid strain is sufficient to cause G2/M arrest (Sandell and Zakian, 1993). However these cells are not permanently arrested. After 8–12 h, they resume progression through the cell cycle (Sandell and Zakian, 1993). This process was called adaptation because the cells resumed the cell cycle while the DNA damage signal was still present (Sandell and Zakian, 1993; Toczyski *et al.*, 1997; Lee *et al.*, 1998b). Adaptation is accompanied by disappearance of Rad53p phosphorylation (Pellicioli *et al.*, 2001).

The transient arrest followed by adaptation would not be expected to block the growth of a telomerase-null culture. However, a more permanent arrest is found when there are multiple sites of DNA damage. Cells that have two DSBs induced simultaneously show permanent cell cycle arrest (Lee *et al.*, 1998b). We found that, as telomeres shorten in *tlc1Δ* cultures, G2/M arrest and an induction of Rad53p phosphorylation occurred. It is not known how many dysfunctional telomeres the cell must sense before arresting; however, because the Rad53p phosphorylation remained high, multiple dysfunctional telomeres may be preventing adaptation. During the initial cell divisions, when most telomeres are still long, the *tlc1Δ* cells might adapt to the initial dysfunctional telomere, but with the subsequent burden of additional dysfunctional telomeres, the cells display a more prolonged arrest. This may be similar to the arrest and adaptation seen in *cdc13-1* mutants. Growth of these cells at the nonpermissive temperature initially allows adaptation, but arrest occurs again at G2/M in the next cell-cycle (Toczyski *et al.*, 1997).

This response to multiple short telomeres may be similar to the increased radiosensitivity of mTR−/− mouse embryonic fibroblasts. When telomeres are long, in early genera-

tions, mTR−/− cells show radiosensitivity similar to wild-type cells. However in later generations (mTR−/− G4–G6) when significant telomere shortening has occurred, there is an increased response to ionizing radiation (Goytisolo *et al.*, 2000; Wong *et al.*, 2000). The increased response mimics the response to higher doses of irradiation, suggesting that the dysfunctional telomeres mimic additional double-stranded DNA breaks.

Repair of Dysfunctional Telomeres

Telomerase-null yeast cells may also respond to telomere dysfunction by attempting to repair the damage. This repair can occur through homologous recombination, which ultimately leads to survivors *in S. cerevisiae* (Lundblad and Blackburn, 1993) and may also occur through nonhomologous-end-joining (NHEJ). In both cases, the damage signals from the dysfunctional end would be temporarily eliminated.

In the yeast *Kluyveromyces lactis*, chromosomes with short telomeres undergo higher rates of subtelomeric recombination than those with long telomeres (McEachern and Iyer, 2001; Lundblad, 2002). This suggests that telomere–telomere recombination may be one mechanism to repair loss of telomere function at short telomeres, even before the generation of survivors. In the case of telomerase-null cells, this recombination will have to repair many chromosome ends simultaneously. When many telomeres become short, only those cells that have induced recombination at all telomeres can grow, and these cells likely represent survivors (Lundblad and Blackburn, 1993). Inactivation of the damage recognition pathway in *Δtlc1 Δrad9 Δrad24Δ* or *tlc1Δ mec1Δ sml1Δ* mutants did not affect the rate of survivor generation (Figures 5A and 6A). This suggests that cell cycle arrest is not the limiting step in generation of survivors or that survivors have inactivated the response to DNA-damage checkpoints.

End-to-end chromosome fusion will also eliminate the apparent double-strand break at dysfunctional telomeres and allow cells to overcome checkpoint arrest. This fusion pathway clearly occurs in cells with dysfunctional telomeres (Nakamura *et al.*, 1998; van Steensel *et al.*, 1998; Hackett *et al.*, 2001; Hemann *et al.*, 2001b). However, this mechanism leads to dicentric chromosomes and ultimately to further chromosome breaks and rearrangements (Hackett *et al.*, 2001).

A Function for the DNA Damage Checkpoint in Both Telomere Lengthening and Cell Cycle Arrest

Genes involved in the DNA damage checkpoint are also involved in telomere length maintenance. In *S. pombe*, double mutants in the two ATM homologues *rad3* and *tel1* show telomere shortening similar to telomerase mutants and ultimately generate survivors with circular chromosomes (Naito *et al.*, 1998). Similarly, in *S. cerevisiae* double mutants in both checkpoint genes *MEC1* and *TEL1* display a senescence phenotype analogous to that seen in a telomerase mutant (Ritchie *et al.*, 1999). Telomerase activity is intact in these mutants; however, access of telomerase to the telomere is impaired (Chan *et al.*, 2001). In wild-type cells telomerase is targeted to the shortest telomeres (Marcand *et al.*, 1999; Hemann *et al.*, 2001b; Hathcock *et al.*, 2002). Because ATM homologues are clearly involved in allowing telomerase ac-

Figure 7 (facing page). Accumulation of G$_2$/M-arrested cells in *tlc1Δ* cells does not depend on *TEL1* and *MAD2*. (A) Growth potential assay for wild-type (◇), *tlc1Δ* (●) and *tlc1Δ tel1Δ* cells (filled triangles). (B) Growth potential assay for wild-type (◇), *tlc1Δ* (●) and *tlc1Δ mad2Δ* cells (◆). (C) Quantitation of cell cycle distribution of DAPI-stained cells. Wild-type (white bars), *tlc1Δ* (black bars) and *tlc1Δ tel1Δ* (hatched bars) cells. Cells were divided into different cell cycle stages as depicted at the bottom of the graphs. (D) Quantitation of cell cycle distribution of DAPI-stained cells. Wild-type (white bars), *tlc1Δ* (black bars) and *tlc1Δ mad2Δ* (waved bars) cells. Cells were divided into different cell cycle stages as depicted at the bottom of the graphs. Wild-type cells are only shown for first and last day of both experiments but showed similar profiles for the other days that were tested. The data shown for each mutant is derived from the analysis of one mutant spore. Another isolate that was analyzed for each mutant gave similar results.
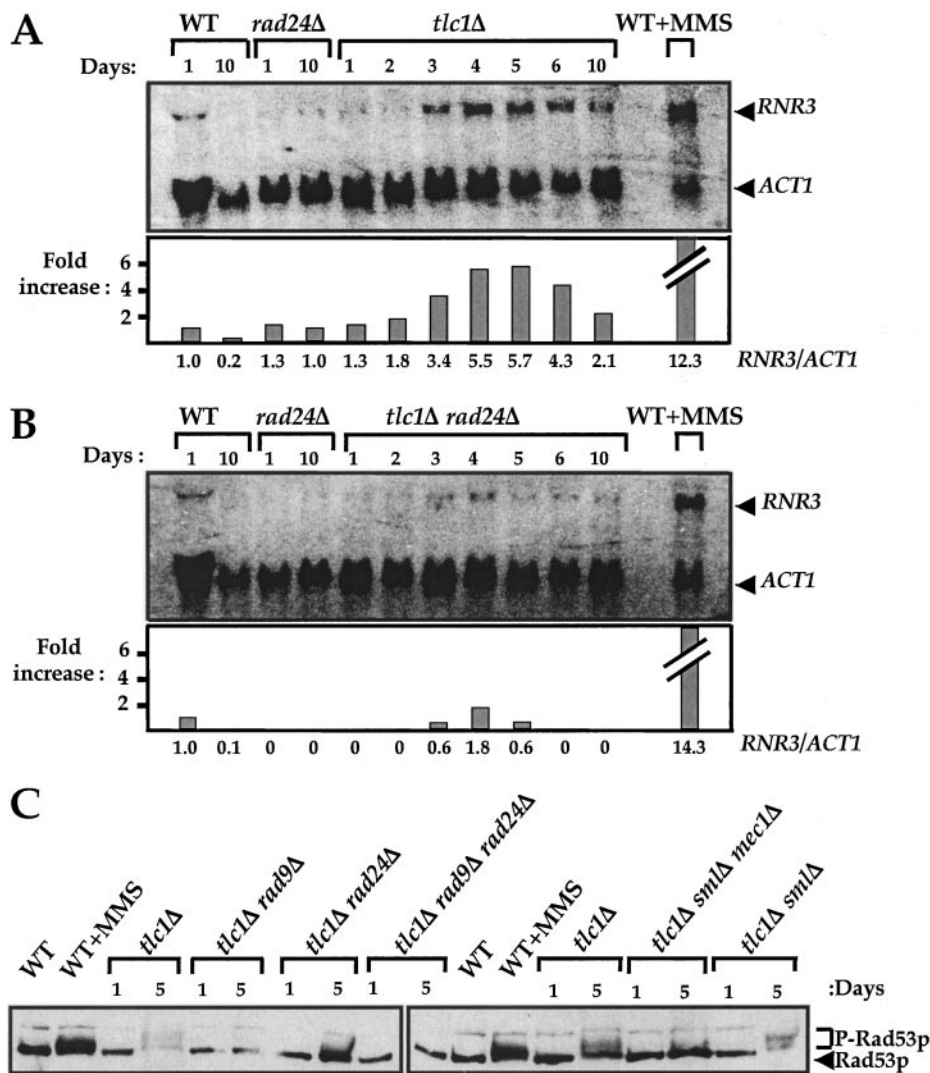
Figure 8. RNR3 mRNA induction and Rad53p phosphorylation in *tlc1Δ* cells. (A) Northern blot analysis was performed for the induction of *RNR3* mRNA in *tlc1Δ* and (B) *tlc1Δ rad24Δ* cells at different days of the growth potential assay (see Figure 4A). The *ACT1* mRNA signal was used to normalize the *RNR3* mRNA signal. As a positive control for *RNR3* induction wild-type cells were treated with 0.04% MMS for 2 h. Quantitation of the signal is plotted below the blot. (C) Rad53p phosphorylation was assayed by Western blot. Rad53p is indicated by an arrow and phosphorylated species of Rad53p are indicated by the bracket. Cells from day 1 and day 5 of the growth potential assay (Figures 5A and 6A) were analyzed. As a positive control for Rad53p phosphorylation wild-type cells were treated with 0.04% MMS for 2 h with 1 h recovery.

cess to telomeres, these genes may be involved in the elongation of short telomeres. Thus, even in the absence of telomere dysfunction, the ATM DNA damage pathway may be involved in sensing short telomeres and allowing their elongation.

If the ATM checkpoint is normally activated to signal elongation of short telomeres, how do short dysfunctional telomeres send a signal through this same pathway that results in G2/M arrest? Perhaps a large number of short telomeres sends a strong enough signal that will activate an arrest, as described above for overcoming adaptation to arrest. Alternatively, the persistence of short telomeres after G2/M, when telomerase elongation may occur (Diede and Gottschling, 1999), may send a qualitatively different signal that results in arrest in the next cell cycle. It is also possible that there are specific proteins that are bound at dysfunctional telomeres and that the ATM pathway responds differently, depending on whether these proteins are present at telomeres or not. Understanding how dysfunctional telo-

meres signal cell cycle arrest will be an exciting challenge for the future.

ACKNOWLEDGMENTS

REFERENCES

Allen, J.B., Zhou, Z., Siede, W., Friedberg, E.C., and Elledge, S.J. (1994). The SAD1/RAD53 protein kinase controls multiple checkpoints and DNA damage-induced transcription in yeast. Genes Dev. 8, 2401–2415.

Blasco, M.A., Lee, H.-W., Hande, P.M., Samper, E., Lansdorp, P.M., DePinho, R.A., and Greider, C.W. (1997). Telomere shortening and tumor formation by mouse cells lacking telomerase RNA. Cell *91*, 25–34.

Brachmann, C.B., Davies, A., Cost, G.J., Caputo, E., Li, J., Hieter, P., and Boeke, J.D. (1998). Designer deletion strains derived from *Saccharomyces cerevisiae* S288C: a useful set of strains and plasmids for PCR-mediated gene disruption and other applications. Yeast *14*, 115–132.

Chan, S.W., Chang, J., Prescott, J., and Blackburn, E.H. (2001). Altering telomere structure allows telomerase to act in yeast lacking ATM kinases. Curr. Biol. *11*, 1240–1250.

Charles, J.F., Jaspersen, S.L., Tinker-Kulberg, R.L., Hwang, L., Szidon, A., and Morgan, D.O. (1998). The Polo-related kinase Cdc5 activates and is destroyed by the mitotic cyclin destruction machinery in *S. cerevisiae*. Curr. Biol. *8*, 497–507.

Chen, Q., IJpma, A., and Greider, C.W. (2001). Two survivor pathways that allow growth in the absence of telomerase are generated by distinct telomere recombination events. Mol. Cell. Biol. *21*, 1819–1827.

Cheng, L., Hunke, L., and Hardy, C.F. (1998). Cell cycle regulation of the *Saccharomyces cerevisiae* polo-like kinase cdc5p. Mol. Cell. Biol. *18*, 7360–7370.

Chin, L., Artandi, S., Shen, Q., Tam, S., Lee, S.-L., Gottlieb, G., Greider, C.W., and DePinho, R.A. (1999). p53 deficiency rescues the adverse effects of telomere loss in vivo and cooperates with telomere dysfunction to accelerate carcinogenesis. Cell *97*, 527–538.

Collart, M.A., and Oliviero, S. (1993). Preparation of yeast RNA. John Wiley & Sons, Inc., New York.

Connelly, C., and Hieter, P. (1996). Budding yeast SKP1 encodes an evolutionarily conserved kinetochore protein required for cell cycle progression. Cell *86*, 275–285.

D'Amours, D., and Jackson, S.P. (2001). The yeast Xrs2 complex functions in S phase checkpoint regulation. Genes Dev. *15*, 2238–2249.

de la Torre-Ruiz, M.A., Green, C.M., and Lowndes, N.F. (1998). RAD9 and RAD24 define two additive, interacting branches of the DNA damage checkpoint pathway in budding yeast normally required for Rad53 modification and activation. EMBO J. *17*, 2687–2698.

de Lange, T. (2002). Protection of mammalian telomeres. Oncogene *21*, 532–540.

Diede, S.J., and Gottschling, D.E. (1999). Telomerase-mediated telomere addition in vivo requires DNA primase and DNA polymerases alpha and delta. Cell *99*, 723–733.

Eckardt-Schupp, F., Siede, W., and Game, J.C. (1987). The RAD24 (= Rs1) gene product of *Saccharomyces cerevisiae* participates in two different pathways of DNA repair. Genetics *115*, 83–90.

Elledge, S.J., and Davis, R.W. (1990). Two genes differentially regulated in the cell cycle and by DNA-damaging agents encode alternative regulatory subunits of ribonucleotide reductase. Genes Dev. *4*, 740–751.

Emili, A. (1998). MEC1-dependent phosphorylation of Rad9p in response to DNA damage. Mol Cell *2*, 183–189.

Enomoto, S., Glowczewski, L., and Berman, J. (2002). MEC3, MEC1, and DDC2 are essential components of a telomere checkpoint pathway required for cell cycle arrest during senescence in *Saccharomyces cerevisiae*. Mol. Biol. Cell *13*, 2626–2638.

Evans, S.K., and Lundblad, V. (1999). Est1 and Cdc13 as comediators of telomerase access. Science *286*, 117–120.

Feinberg, A.P., and Vogelstein, B. (1983). A technique for radiolabeling DNA restriction endonuclease fragments to high specific activity. Anal. Biochem. *132*, 6–13.

Gardner, R., Putnam, C.W., and Weinert, T. (1999). RAD53, DUN1 and PDS1 define two parallel G2/M checkpoint pathways in budding yeast. EMBO J. *18*, 3173–3185.

Garvik, B., Carson, M., and Hartwell, L. (1995). Single-stranded DNA arising at telomeres in cdc13 mutants may constitute a specific signal for the RAD9 checkpoint. Mol. Cell. Biol. *15*, 6128–6138.

Goldstein, A.L., and McCusker, J.H. (1999). Three new dominant drug resistance cassettes for gene disruption in *Saccharomyces cerevisiae*. Yeast *15*, 1541–1553.

Goytisolo, F.A., Samper, E., Martin-Caballero, J., Finnon, P., Herrera, E., Flores, J.M., Bouffler, S.D., and Blasco, M.A. (2000). Short telomeres result in organismal hypersensitivity to ionizing radiation in mammals. J. Exp. Med. *192*, 1625–1636.

Grandin, N., Damon, C., and Charbonneau, M. (2001). Ten1 functions in telomere end protection and length regulation in association with Stn1 and Cdc13. EMBO J. *20*, 1173–1183.

Grandin, N., Reed, S.I., and Charbonneau, M. (1997). Stn1, a new *Saccharomyces cerevisiae* protein, is implicated in telomere size regulation in association with Cdc13. Genes Dev. *11*, 512–527.

Green, C.M., Erdjument-Bromage, H., Tempst, P., and Lowndes, N.F. (2000). A novel Rad24 checkpoint protein complex closely related to replication factor C. Curr. Biol. *10*, 39–42.

Greider, C.W. (1996). Telomere length regulation. Annu. Rev. Biochem. *65*, 337–365.

Greider, C.W., and Blackburn, E.H. (1985). Identification of a specific telomere terminal transferase activity in *Tetrahymena* extracts. Cell *43*, 405–413.

Grenon, M., Gilbert, C., and Lowndes, N.F. (2001). Checkpoint activation in response to double-strand breaks requires the Mre11/Rad50/Xrs2 complex. Nat. Cell Biol. *3*, 844–847.

Hackett, J.A., Feldser, D.M., and Greider, C.W. (2001). Telomere dysfunction increases mutation rate and genomic instability. Cell *106*, 275–286.

Hartwell, L.H. (1974). *Saccharomyces cerevisiae* cell cycle. Bacteriol. Rev. *38*, 164–198.

Hathcock, K.S., Hemann, M.T., Opperman, K.K., Strong, M.A., Greider, C.W., and Hodes, R.J. (2002). Haploinsufficiency of mTR results in defects in telomere elongation. Proc. Natl. Acad. Sci. USA *99*, 3591–3596.

Hegemann, J.H., Shero, J.H., Cottarel, G., Philippsen, P., and Hieter, P. (1988). Mutational analysis of centromere DNA from chromosome VI of *Saccharomyces cerevisiae*. Mol. Cell Biol. *8*, 2523–2535.

Hemann, M.T., Hackett, J., IJpma, A., and Greider, C.W. (2000). Telomere length, telomere binding proteins and DNA damage signaling. Cold Spring Harbor Laboratory Symp. Quant. Biol. *LXV*, 275–279.

Hemann, M.T., Rudolph, K.L., Strong, M.A., DePinho, R.A., Chin, L., and Greider, C.W. (2001a). Telomere dysfunction triggers developmentally regulated germ cell apoptosis. Mol. Biol. Cell *12*, 2023–2030.

Hemann, M.T., Strong, M.A., Hao, L.Y., and Greider, C.W. (2001b). The shortest telomere, not average telomere length, is critical for cell viability and chromosome stability. Cell *107*, 67–77.

Hieter, P., Mann, C., Snyder, M., and Davis, R.W. (1985). Mitotic stability of yeast chromosomes: a colony color assay that measures nondisjunction and chromosome loss. Cell *40*, 381–392.

Hughes, T.R., Weilbaecher, R.G., Walterscheid, M., and Lundblad, V. (2000). Identification of the single-strand telomeric DNA binding

domain of the *Saccharomyces cerevisiae* Cdc13 protein. Proc. Natl. Acad. Sci. USA *97*, 6457–6462.

Hyland, K.M., Kingsbury, J., Koshland, D., and Hieter, P. (1999). Ctf19p: a novel kinetochore protein in *Saccharomyces cerevisiae* and a potential link between the kinetochore and mitotic spindle. J. Cell Biol. *145*, 15–28.

Johnson, F.B., Marciniak, R.A., McVey, M., Stewart, S.A., Hahn, W.C., and Guarente, L. (2001). The *Saccharomyces cerevisiae* WRN homolog Sgs1p participates in telomere maintenance in cells lacking telomerase. EMBO J. *20*, 905–913.

Karlseder, J., Broccoli, D., Dai, Y., Hardy, S., and de Lange, T. (1999). p53- and ATM-dependent apoptosis induced by telomeres lacking TRF2. Science *283*, 1321–1325.

Kirk, K.E., Harmon, B.P., Reichardt, I.K., Sedat, J.W., and Blackburn, E.H. (1997). Block in anaphase chromosome separation caused by a telomerase template mutation. Science *275*, 1478–1481.

Kohli, J., Hottinger, H., Munz, P., Strauss, A., and Thuriaux, P. (1977). Genetic mapping in *Schizosaccharomyces pombe* by mitotic and meiotic analysis and induced haploidization. Genetics *87*, 471–489.

Kondo, T., Matsumoto, K., and Sugimoto, K. (1999). Role of a complex containing Rad17, Mec3, and Ddc1 in the yeast DNA damage checkpoint pathway. Mol. Cell. Biol. *19*, 1136–1143.

Kondo, T., Wakayama, T., Naiki, T., Matsumoto, K., and Sugimoto, K. (2001). Recruitment of mec1 and ddc1 checkpoint proteins to double-strand breaks through distinct mechanisms. Science *294*, 867–870.

Le, S., Moore, J.K., Haber, J.E., and Greider, C.W. (1999). *RAD51 and RAD50* define two pathways that collaborate to maintain telomeres in the absence of telomerase. Genetics *152*, 143–152.

Lee, H.-W., Blasco, M.A., Gottlieb, G.J., Horner, J.W., Greider, C.W., and DePinho, R.A. (1998a). Essential role of mouse telomerase in highly proliferative organs. Nature *392*, 569–574.

Lee, S.E., Moore, J.K., Holmes, A., Umezu, K., Kolodner, R.D., and Haber, J.E. (1998b). Saccharomyces Ku70, mre11/rad50 and RPA proteins regulate adaptation to G2/M arrest after DNA damage. Cell *94*, 399–409.

Lendvay, T.S., Morris, D.K., Sah, J., Balasubramanian, B., and Lundblad, V. (1996). Senescence mutants of *Saccharomyces cerevisiae* with a defect in telomere replication identify three additional EST genes. Genetics *144*, 1399–1412.

Lin, J.J., and Zakian, V.A. (1996). The Saccharomyces CDC13 protein is a single-strand TG1–3 telomeric DNA-binding protein in vitro that affects telomere behavior in vivo. Proc. Natl. Acad. Sci. USA *93*, 13760–13765.

Lingner, J., Cech, T.R., Hughes, T.R., and Lundblad, V. (1997a). Three ever shorter telomere (EST) genes are dispensable for in vitro yeast telomerase activity. Proc. Natl. Acad. Sci. USA *94*, 11190–11195.

Lingner, J., Hughes, T.R., Shevchenko, A., Mann, M., Lundblad, V., and Cech, T.R. (1997b). Reverse transcriptase motifs in the catalytic subunit of telomerase. Science *276*, 561–567.

Lundblad, V. (2002). Telomere maintenance without telomerase. Oncogene *21*, 522–531.

Lundblad, V., and Blackburn, E.H. (1993). An alternative pathway for yeast telomere maintenance rescues *est1*-senescence. Cell *73*, 347–360.

Lundblad, V., and Szostak, J.W. (1989). A mutant with a defect in telomere elongation leads to senescence in yeast. Cell *57*, 633–643.

Lydall, D., and Weinert, T. (1995). Yeast checkpoint genes in DNA damage processing: implications for repair and arrest. Science *270*, 1488–1491.

Lydall, D., and Weinert, T. (1997). G2/M checkpoint genes of *Saccharomyces cerevisiae*: further evidence for roles in DNA replication and/or repair. Mol. Gen. Genet. *256*, 638–651.

Marcand, S., Brevet, V., and Gilson, E. (1999). Progressive cis-inhibition of telomerase upon telomere elongation. EMBO J. *18*, 3509–3519.

McEachern, M.J., and Iyer, S. (2001). Short telomeres in yeast are highly recombinogenic. Mol. Cell *7*, 695–704.

Melo, J., and Toczyski, D. (2002). A unified view of the DNA-damage checkpoint. Curr. Opin. Cell Biol. *14*, 237–245.

Melo, J.A., Cohen, J., and Toczyski, D.P. (2001). Two checkpoint complexes are independently recruited to sites of DNA damage in vivo. Genes Dev. *15*, 2809–2821.

Mortimer, R.K., Contopoulou, R., and Schild, D. (1981). Mitotic chromosome loss in a radiation-sensitive strain of the yeast *Saccharomyces cerevisiae*. Proc. Natl. Acad. Sci. USA *78*, 5778–5782.

Naito, T., Matsuura, A., and Ishikawa, F. (1998). Circular chromosome formation in a fission yeast mutant defective in two ATM homologues. Nat. Genet. *20*, 203–206.

Nakamura, T.M., Cooper, J.P., and Cech, T.R. (1998). Two modes of survival of fission yeast without telomerase. Science *282*, 493–496.

Nugent, C.I., Hughes, T.R., Lue, N.F., and Lundblad, V. (1996). Cdc13p: a single-strand telomeric DNA-binding protein with a dual role in yeast telomere maintenance. Science *274*, 249–252.

Pellicioli, A., Lee, S.E., Lucca, C., Foiani, M., and Haber, J.E. (2001). Regulation of *Saccharomyces* Rad53 checkpoint kinase during adaptation from DNA damage-induced G2/M arrest. Mol. Cell *7*, 293–300.

Pellicioli, A., Lucca, C., Liberi, G., Marini, F., Lopes, M., Plevani, P., Romano, A., Di Fiore, P.P., and Foiani, M. (1999). Activation of Rad53 kinase in response to DNA damage and its effect in modulating phosphorylation of the lagging strand DNA polymerase. EMBO J. *18*, 6561–6572.

Pennock, E., Buckley, K., and Lundblad, V. (2001). Cdc13 delivers separate complexes to the telomere for end protection and replication. Cell *104*, 387–396.

Qi, H., and Zakian, V.A. (2000). The Saccharomyces telomere-binding protein Cdc13p interacts with both the catalytic subunit of DNA polymerase alpha and the telomerase-associated est1 protein. Genes Dev. *14*, 1777–1788.

Ritchie, K.B., Mallory, J.C., and Petes, T.D. (1999). Interactions of TLC1 (which encodes the RNA subunit of telomerase), TEL1, and MEC1 in regulating telomere length in the yeast *Saccharomyces cerevisiae*. Mol. Cell. Biol. *19*, 6065–6075.

Ritchie, K.B., and Petes, T.D. (2000). The Mre11p/Rad50p/Xrs2p complex and the Tel1p function in a single pathway for telomere maintenance in yeast. Genetics *155*, 475–479.

Rose, M.D., Winston, F., and Hieter, P. (1990). Methods in yeast genetics. A laboratory course manual. Cold Spring Harbor, New York: Cold Spring Harbor Laboratory Press.

Rouse, J., and Jackson, S.P. (2002). Interfaces between the detection, signaling, and repair of DNA damage. Science *297*, 547–551.

Sanchez, Y., Bachant, J., Wang, H., Hu, F., Liu, D., Tetzlaff, M., and Elledge, S.J. (1999). Control of the DNA damage checkpoint by chk1 and rad53 protein kinases through distinct mechanisms. Science *286*, 1166–1171.

Sanchez, Y., Desany, B.A., Jones, W.J., Liu, Q., Wang, B., and Elledge, S.J. (1996). Regulation of RAD53 by the ATM-like kinases MEC1 and TEL1 in yeast cell cycle checkpoint pathways. Science *271*, 357–360.

Sandell, L.L., and Zakian, V.A. (1993). Loss of a yeast telomere: arrest, recovery, and chromosome loss. Cell *75*, 729–739.

Schiestl, R.H., and Gietz, R.D. (1989). High efficiency transformation of intact yeast cells using single stranded nucleic acids as a carrier. Curr. Genet. *16*, 339–346.

Schupbach, M. (1971). The isolation and genetic classification of UV-sensitive mutants of *Schizosaccharomyces pombe*. Mutat. Res. *11*, 361–371.

Schwartz, M.F., Duong, J.K., Sun, Z., Morrow, J.S., Pradhan, D., and Stern, D.F. (2002). Rad9 phosphorylation sites couple Rad53 to the *Saccharomyces cerevisiae* DNA damage checkpoint. Mol. Cell *9*, 1055–1065.

Shimomura, T., Ando, S., Matsumoto, K., and Sugimoto, K. (1998). Functional and physical interaction between Rad24 and Rfc5 in the yeast checkpoint pathways. Mol. Cell. Biol. *18*, 5485–5491.

Singer, M.S., and Gottschling, D.E. (1994). *TLC1*: template RNA component of *Saccharomyces cerevisiae* telomerase. Science *266*, 404–409.

Soulier, J., and Lowndes, N.F. (1999). The BRCT domain of the *S. cerevisiae* checkpoint protein Rad9 mediates a Rad9-Rad9 interaction after DNA damage. Curr. Biol. *9*, 551–554.

Spencer, F., Gerring, S.L., Connelly, C., and Hieter, P. (1990). Mitotic chromosome transmission fidelity mutants in *Saccharomyces cerevisiae*. Genetics *124*, 237–249.

Sun, Z., Fay, D.S., Marini, F., Foiani, M., and Stern, D.F. (1996). Spk1/Rad53 is regulated by Mec1-dependent protein phosphorylation in DNA replication and damage checkpoint pathways. Genes Dev. *10*, 395–406.

Sun, Z., Hsiao, J., Fay, D.S., and Stern, D.F. (1998). Rad53 FHA domain associated with phosphorylated Rad9 in the DNA damage checkpoint. Science *281*, 272–274.

Teng, S., Chang, J., McCowan, B., and Zakian, V.A. (2000). Telomerase-independent lengthening of yeast telomeres occurs by an abrupt Rad50p-dependent, Rif-inhibited recombinational process. Mol. Cell *6*, 947–952.

Teng, S.C., and Zakian, V.A. (1999). Telomere-telomere recombination is an efficient bypass pathway for telomere maintenance in *Saccharomyces cerevisiae*. Mol. Cell. Biol. *19*, 8083–8093.

Toczyski, D.P., Galgoczy, D.J., and Hartwell, L.H. (1997). CDC5 and CKII control adaptation to the yeast DNA damage checkpoint. Cell *90*, 1097–1106.

Tsai, Y.L., Tseng, S.F., Chang, S.H., Lin, C.C., and Teng, S.C. (2002). Involvement of replicative polymerases, tel1p, mec1p, cdc13p, and the ku complex in telomere-telomere recombination. Mol. Cell. Biol. *22*, 5679–5687.

Usui, T., Ogawa, H., and Petrini, J.H. (2001). A DNA damage response pathway controlled by Tel1 and the Mre11 complex. Mol Cell *7*, 1255–1266.

van Steensel, B., Smogorzewska, A., and de Lange, T. (1998). TRF2 protects human telomeres from end-to-end fusions. Cell *92*, 401–413.

Venclovas, C., and Thelen, M.P. (2000). Structure-based predictions of Rad1, Rad9, Hus1 and Rad17 participation in sliding clamp and clamp-loading complexes. Nucleic Acids Res. *28*, 2481–2493.

Weinert, T.A., and Hartwell, L.H. (1988). The RAD9 gene controls the cell cycle response to DNA damage in *Saccharomyces cerevisiae*. Science *241*, 317–322.

Winzeler, E.A. *et al.* (1999). Functional characterization of the *S. cerevisiae* genome by gene deletion and parallel analysis. Science *285*, 901–906.

Wong, K.K. *et al.* (2000). Telomere dysfunction impairs DNA repair and enhances sensitivity to ionizing radiation. Nat. Genet. *26*, 85–88.

Zakian, V.A. (1989). Structure and function of telomeres. Annu. Rev. Genet. *23*, 579–604.

Zhou, B.B., and Elledge, S.J. (2000). The DNA damage response: putting checkpoints in perspective. Nature *408*, 433–439.